Clin Exp Nephrol (2015) 19:771–782
DOI 10.1007/s10157-014-1063-1

ORIGINAL ARTICLE

pH-sensitive expression of calcium-sensing receptor (CaSR) in type-B intercalated cells of the cortical collecting ducts (CCD) in mouse kidney

Yukiko Yasuoka · Yuichi Sato · Jillian M. Healy · Hiroshi Nonoguchi · Katsumasa Kawahara

Received: 4 September 2014 / Accepted: 22 November 2014 / Published online: 13 December 2014

Abstract
Background The localization and role of the calcium-sensing receptor (CaSR) along the nephron including the collecting ducts is still open to debate.
Methods Using the quantitative, highly sensitive in situ hybridization technique and a double-staining immunohistochemistry technique, we investigated the axial distribution and expression of CaSR along the nephron in mice (C57B/6J) treated for 6 days with acid or alkali diets.
Results Under control condition, CaSR was specifically localized in the cortical and medullary thick ascending limb of Henle's loop (CTAL and MTAL), macula densa (MD), distal convoluted tubule (DCT), and CCD (TALs, MD > DCT, CCD). Along the CCD, CaSR was co-localized with an anion exchanger type 4 (AE4), a marker of the basolateral membrane of type-B intercalated cell (IC-B) in mice. On the contrary, CaSR was not detected either in principal cells (PC) or in type-A intercalated cell (IC-A). CaSR expression levels in IC-B significantly ($P < 0.005$) decreased when mice were fed NH_4Cl (acid) diets and increased when animals were given $NaHCO_3$ (alkali) diets. As expected, cell heights of IC-A and IC-B significantly ($P < 0.005$) increased in the above experimental conditions. Surprisingly, single infusion (ip) of neomycin, an agonist of CaSR, significantly ($P < 0.005$) increased urinary Ca excretion without further increasing the hourly urine volume and significantly ($P < 0.05$) decreased urine pH.
Conclusion CaSR, cloned from rat kidney, was localized in the basolateral membrane of IC-B and was more expressed during alkali-loading. Its alkali-sensitive expression may promote urinary alkali secretion for body acid–base balance.

Keywords Calcium-sensing receptor · Neomycin · Urinary calcium concentration · Acid/base diet · Kidney collecting duct intercalated cell

Y. Yasuoka · K. Kawahara (✉)
Department of Physiology, Kitasato University School of Medicine, 1-15-1 Kitasato, Minami-ku, Sagamihara 252-0374, Japan
e-mail: kawahara@kitasato-u.ac.jp

Y. Yasuoka · K. Kawahara
Department of Cellular and Molecular Physiology, Kitasato University Graduate School of Medical Sciences, Sagamihara 252-0374, Japan

Y. Sato
Department of Molecular Diagnostics, Kitasato University School of Allied Health Sciences, Sagamihara 252-0374, Japan

J. M. Healy
ALESS Program, Komaba Organizational for Educational Excellence, College of Art and Sciences, The University of Tokyo, 3-8-1 Komaba, Meguro-ku, Tokyo 153-8902, Japan

H. Nonoguchi
Division of Internal Medicine, Kitasato University Medical Center, 6-100 Arai, Kitamoto 364-8501, Japan

Introduction

The kidney plays key roles in water, electrolyte, and pH homeostasis by regulating tubular transport as well as glomerular filtrate [1, 2]. The distal part of the nephron including the collecting ducts (CD) performs the final adjustment to urine before excretion. The expression and activity of various transporters mediating these processes are regulated by specific hormones and, more directly, extracellular ionic and pH changes [3]. Regulating the tubular reabsorption of Ca^{2+} from the filtrate is crucial to Ca^{2+} and pH homeostasis in animals [4].

The calcium-sensing receptor (CaSR), originally cloned from bovine parathyroid glands by Brown et al. [5], plays important roles in body Ca homeostasis via the kidney as well as regulation of plasma Ca concentrations via secretion of parathyroid hormone (PTH) [6–8]. Using an approach based on homology to bovine parathyroid CaSR, Riccardi et al. [9, 10] cloned and characterized rat kidney CaSR (RaKCaR). Soon after reports of CaSR expression on the apical membrane of rat kidney inner medullary CD (IMCD) [11, 12], Riccardi et al. [13] asserted that the RaKCaR mRNA and protein was expressed in the proximal convoluted and straight tubules (PCT and PST, respectively), medullary and cortical thick ascending limb of Henle's loops (MTAL and CTAL, respectively), distal convoluted tubule (DCT) and the cortical CD (CCD). These results were inconsistent with the observations reported by Schnermann and his colleagues [14] using RT-PCR: CaSR (RaKCaR) mRNA was found in MTAL, CTAL, the macula densa (MD) containing segment, and DCT, and, to a lesser extent, in CCD. It was not found in glomeruli, PCT, PST, outer medullary CD (OMCD), and IMCD. To further complicate matters, other studies recently showed no detectable expression of the CaSR protein in the PCT, DCT, or CDs [15, 16], although functional acidification via stimulation of CaSR was independently reported in the CCD from mouse kidney [17].

Thus, using the highly sensitive in situ hybridization with tyramide signal amplification (ISH-TSA) [18, 19] and a double-staining immunohistochemistry (IHC) technique [20], we investigated the localization of CaSR mRNA and protein along the mouse kidney nephron including the CD. The CCD comprises at least three different types of the cells, including principal cells (PC) and type-A and B intercalated cells (IC-A and IC-B, respectively) [21, 22]. In the CCD, Na and water reabsorption and K secretion are primarily conducted by PC, whereas acid (proton) and alkali (bicarbonate) excretion into the urine are the specific domains of the IC-A and IC-B, respectively.

In the present study we found that the CaSR was expressed in the basolateral membrane of IC-B through the CCD as well as in MTAL, CTAL, and MD. Therefore, we further investigated the dietary effects of acid/base loading on the expression of CaSR in the CCD, especially in IC-B. CaSR in IC-B may function as a pH-sensing protein expressed in the kidney distal nephron [23]. Moreover, we investigated time-dependent changes in the urine pH and electrolytes after single infusion (ip) of neomycin, an agonist of the CaSR [9] or of furosemide, an inhibitor of NKCC2 (Na^+–K^+–$2Cl^-$ cotransporter). It is important to elucidate the role of the CaSR expressed in the basolateral membrane of IC-B in the CCD for acid–base balance.

Materials and methods

Laboratory animals

Animal experiments were conducted in accordance with the Kitasato University Guide for the Care and Use of Laboratory Animals and were approved by the Institutional Animal Care and Use Committee (Approval No. 2011-133, 2012-143, 2013-004). C57BL/6J mice (10–12weeks of age) were purchased from Charles River Japan (Yokohama). Mice were acclimated to a laboratory diet with food and water available ad libitum. The total number of animals used in the present study was 62.

Experimental protocol

Mice were placed in individual cages and were given for 6 days either 2.5 % NH_4Cl added to their standard diet or 0.28 M $NaHCO_3$ added to their drinking water of 2 % sucrose solution in accordance with the protocol described previously [24, 25]. Twenty four-hour urine was collected from mice placed in individual metabolic cages 1 day before the end of the acid/base loading (6 days).

In the next series of experiments, normal mice were given drinking water of 1 % glucose solution for hourly urine collection by pipetts. They were also treated with 1 % glucose solution for 24 h before single-injection (12.9 μl/g body wt (bw), ip) of saline (control), furosemide (50 mg/kg bw, Sanofi-Aventis, Paris, France) or neomycin (43 mg/kg bw, Sigma-Aldrich, St Louis, USA). This procedure was successful for hourly urine collection, although there was no significant difference in urine flow between the two groups (tap water: 0.14 ± 0.02 μl/h, $n = 3$; 1 % glucose drinking: 0.16 ± 0.04 μl/h, $n = 5$). Further, in preliminary experiments, we found no glucosuria in mice treated with tap-water containing 5 % glucose for 1 day ($n = 5$).

Tissue collection

For ISH and IHC studies, mice were anesthetized with pentobarbital sodium salt (37.5 mg/kg bw, ip). The kidneys were quickly removed and cut longitudinally. Main kidney pieces were fixed by immersion in ice-cold 4 % paraformaldehyde/0.1 M phosphate buffer overnight and processed in paraffin for histological analysis.

Blood and urine samples

For blood analysis, heparinized blood was collected from the carotid artery of mice anesthetized with 1.5 % isoflurane in 30 % O_2 (a mixture of 100 % O_2 and air). The gas status and electrolytes of collected urine and blood

samples were analyzed immediately on a Radiometer ABL505 blood gas analyzer (Radiometer, Copenhagen, Denmark). The calcium levels of blood and urine were assessed by direct colorimetric determination according to the manual of calcium *E* Test Wako (Wako Pure Chemical, Osaka). Urinary phosphate (Pi) and magnesium (Mg) levels were assessed by direct colorimetric determination according to the manual of Phosphor *C* Test Wako and Magnesium *B* Test Wako (Wako Pure Chemical).

Immunohistochemistry

The 3-μm kidney sections of paraffin-embedded tissue were deparaffinized and immunostained as described previously [20, 26]. Briefly, the sections were blocked with 5 % normal goat serum reacted with a mouse monoclonal anti human CaSR antibody [15, 27] (1:500, MA1-934; Thermo scientific, Rockford, USA; formerly Affinity BioReagents) and followed by Histofine Simple Stain Mouse MAX-PO (Nichirei Bioscience, Tokyo). The antibody was characterized and specified in the previous manuscript [15]. Stainings were visualized using DAB liquid System (Bio SB, Santa Barbara, USA) and counterstained with Mayer's hematoxylin (Muto Pure Chemicals, Tokyo).

Double immunofluorescence labeling

We identified intrasegmental heterogeneity of the CD using a double immunofluorescence labeling technique with a rabbit polyclonal anti rat AQP2 antibody (1:1,000; Alpha Diagnostic, San Antonio, USA) [26], a rabbit polyclonal anti rat AE1 antibody (1:500; Alpha Diagnostic) [28], a rabbit polyclonal anti human AE4 antibody (1:500; Alpha Diagnostic) [28], and a monoclonal anti human CaSR antibody (1:500, Thermo Scientific) as described previously [20]. For all antibodies, negative controls were used in which the primary antibody was omitted.

In situ hybridization

From the total RNA of mouse kidney (BD Bioscience, Franklin Lakes, USA), a 511-bp fragment (Genbank; NM_013803, 526–1036) of mouse CaSR cDNA was obtained by RT-PCR. Digoxigenin-labeled cRNA probes were prepared from 50 ng PCR products using a DIG (digoxigenin) RNA labeling Kit (Roche Diagnostics, Mannheim, Germany), and ISH-TSA was performed according to the method described previously [19, 29]. The hybridized sections from C57BL/6J mice kidneys were successively treated with 0.1 % avidin and 0.01 % biotin solutions to block false-positive signals due to the reactivity of endogenous biotin (biotin blocking system, DakoCytomation, Glostrup, Denmark). After rinsing in TBS-T (0.01 mol/L Tris-HCl, pH 7.5; 300 mmol/L NaCl, 0.5 % Tween-20), the sections were incubated in 0.5 % casein/TBS (0.01 mol/L Tris-HCl pH 7.5, 150 mmol/L NaCl) for 10 min, followed by a 1:400 diluted horseradish peroxidase (HRP)-conjugated rabbit anti-DIG F (ab') fragment antibody (DakoCytomation), 0.07 μmol/L biotinylated tyramide solution, and 1:500 diluted HRP-conjugated streptavidin (DakoCytomation), sequentially, at room temperature (25 °C) for 15 min each. Finally, staining was visualized using the DAB liquid System (Bio SB) and counterstained with Mayer's hematoxylin.

Expression of CaSR mRNA and protein was analyzed using a Zeiss microscope equipped with mercury epifluorescence (Axioplan 2, Carl Zeiss, Jena, Germany), and images were obtained using a digital camera (AxioCam MRc5, Carl Zeiss). Captured images were analyzed using an image analysis system (AxioVision Rel. 4.6, Carl Zeiss). Each nephron segment, defined according to the conventional criteria of "The Renal Commission of IUPS" [21], was identified under the microscope (400×) and, if necessary, by segment-specific antibodies as described previously [29].

Counting dots of CaSR mRNA and density of CaSR protein staining

For quantitative analysis of CaSR mRNA expression, the number of brown dots (DAB precipitate) was counted per tubule (50 μm in length) and per cell of each nephron segment [29]. Briefly, for quantitative analysis of CaSR protein expression in the CCD, the fluorescence, measured per cell (membrane and cytosol) except the nuclei, was normalized by the intensity of the corresponding CTAL.

Cell-height measurement

To measure the cell height of PC and IC of the CCD correctively, kidney sections were usually stained with an anti-AQP2 antibody, anti-AE1 antibody, and anti-AE4 antibody. Morphometric evaluation was performed by a single person (Y Yasuoka) who did not know which animals belonged to which groups until after completion of measurement [29].

Statistical analysis

Results are presented as the mean ± SE of the experiments. Statistical analyses were performed with unpaired Student's *t* test and/or the two-way ANOVA. All results with $P < 0.05$ were considered statistically significant.

Results

Expression and localization of the CaSR mRNA along the nephron

Brown dot-like precipitates (0.9–1.4 μm in diameter) indicating CaSR mRNA were detected in some segments along the mouse kidney nephron including the CDs (Fig. 1a–c). The CaSR mRNA was highly expressed in macula densa (MD) (Fig. 1a'), the CTAL and the MTAL (inner stripe) (Fig. 1b, c), and moderately expressed in the DCT and CCD (Fig. 1a', b). Interestingly, the pattern of expression in the CTAL and MTAL was homogeneous, whereas that of the CCD was not even within the same segment. More importantly, no expression was observed in the OMCD (Fig. 1c) or IMCD (figure not shown) as well as in the glomerulus (Fig. 1a), PCT (Fig. 1a), PST (not shown), or thin limbs of Henle's loop (TL) (not shown). In summary, Fig. 1d and e illustrates a unique pattern of the CaSR mRNA expression per tubule and per cell, respectively, along the nephron; high and moderate expression in the middle and distal parts of the nephron, from MTAL to CCD. In the CCD expression, CaSR mRNA was detected only in the specific cell type.

As expected, no hybridization signals were detected when sense probes were used.

Localization of CaSR expression within kidney

Figure 2 shows that DAB-staining IHC signals of CaSR was restricted to renal tubules, such as CTAL, MD, DCT, CCD in the cortex (Fig. 2a, b), and MTAL in the outer medulla (Fig. 2c). Homogeneous, cytoplasmic, and basolateral staining was observed in CTAL and MTAL, whereas much stronger basolateral staining was characteristic in MD (Fig. 2a). Interestingly, DAB-staining was heterogeneous and moderate in CCD (Fig. 2b). No staining was observed in OMCD (Fig. 2c) or TL or IMCD (Fig. 2d). Similar results were obtained from 3 mice (>10 independent sections). This zonal expression pattern in the kidney CDs is consistent with that of Pendrin, a marker of IC-B, which expresses in the cortex, but little in either outer medulla or inner medulla of mouse kidney [30].

Localization of CaSR protein expression in type-B intercalated cell (IC-B)

We further investigated localization of the CaSR protein along the CCD using a double-staining immunohistochemistry technique. As markers of IC-A, IC-B, and PC we chose, in sequence, the basolateral expression of AE1 and AE4, and the apical expression of AQP2. CaSR immunoreactivity (red) was positive only in the CCD cells which were not co-stained with either AQP2 immunoreactivity (green) on the apical membrane of PC (Fig. 3a, a') or AE1 immunoreactivity (green) on the basolateral membrane of IC-A (Fig. 3b, b'). Similar results were obtained from 3 mice. These results suggest that CaSR may be expressed at least either in the IC-B cells or non-A, non-B IC cells of the CCD.

Figure 4 shows that CaSR and AE4 are co-expressed at the basolateral membrane of IC-B in the CCD. Similar results were obtained from 3 mice.

Acid/alkali sensitive expression of CaSR in IC-B

In this series of experiments, we examined mice to determine whether acid/base diets regulated the CaSR mRNA and protein expression in the IC-B of CCD. The blood and urine data are summarized in Tables 1 and 2. Acid/base-induced morphological changes in kidney tubule cells will be discussed in the next heading. First, we counted the number of dots in the CTAL and IC-B under the acid/base loading conditions. Figure 5a–c shows that CaSR mRNA expression in the IC-B decreased and increased, respectively, during NH_4Cl- and $NaHCO_3$-loading, whereas CaSR mRNA expression in the CTAL remained apparently unchanged. Figure 5d, e summarizes the data: although the number of dots remained unchanged in the CTAL (Cont: 2.7 ± 0.3, $+NH_4Cl$: 3.0 ± 0.2, $+NaHCO_3$: 2.9 ± 0.2), it decreased and increased significantly ($P < 0.005$) from 2.4 ± 0.1 (control) to 0.6 ± 0.1 ($+NH_4Cl$) and to 5.2 ± 0.2 ($+NaHCO_3$) in the IC-B, respectively ($n = 10$ tubules each).

Second, we evaluated the intensity of CaSR immunoreactivity in the CTAL and the IC-B of CCD in mice fed acid/base diet. As expected from Fig. 5d, the intensity of CaSR immunoreactivity (red) was high and unchanged in the CTAL (Cont: 242.8 ± 5.0, $+NH_4Cl$: 245.0 ± 5.0, $+NaHCO_3$: 240.4 ± 4.3) ($n = 10$ tubules each) (Fig. 6a–c). On the contrary, CaSR staining in the IC-B apparently decreased and increased in mice fed NH_4Cl (Fig. 6b) and $NaHCO_3$ (Fig. 6c), respectively. In summary, the normalized value of the intensity per tubule (50 μm) in control (45.4 ± 1 % intensity compared with the CTAL) significantly ($P < 0.005$) decreased to 12.2 ± 2 % and increased to 89.6 ± 1.1 % (n = 10 each), respectively, during NH_4Cl (acid)- and $NaHCO_3$ (alkali)-loading (Fig. 6d). Similarly, the normalized value of the intensity per cell in control (34.2 ± 1 % intensity compared with the CTAL) significantly ($P < 0.005$) decreased to 22.2 ± 1 % and increased to 76.1 ± 2 % ($n = 10$ each), respectively (Fig. 6e).

Acid and alkali diet-induced hypertrophy in the CCD

To investigate functional changes of the corresponding nephron segments, we measured the cell-height of the TAL

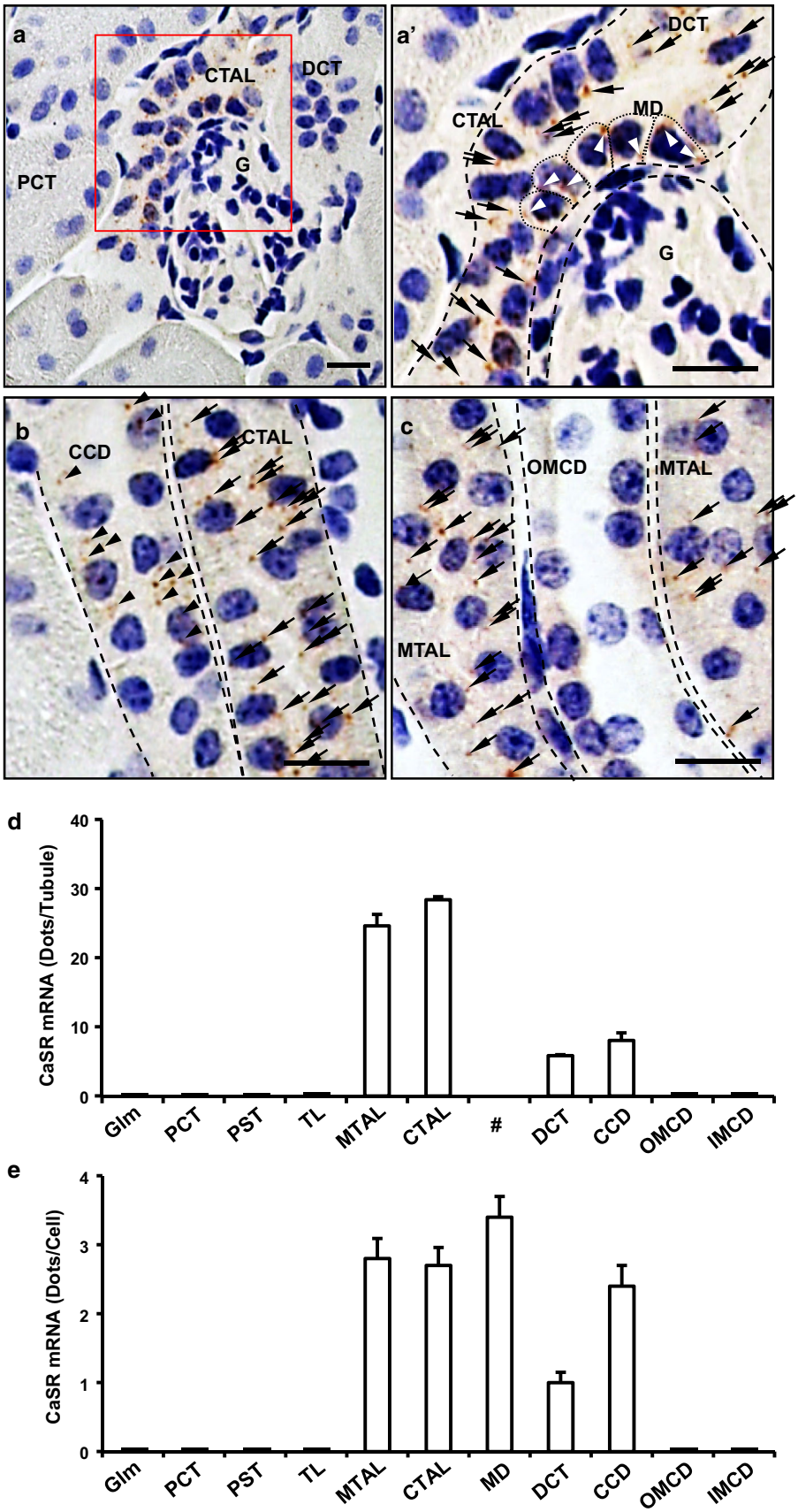

Fig. 1 In situ hybridization of CaSR mRNA in the mouse kidney. **a, a'** CTAL and DCT are observed with strong and moderate signals of CaSR mRNA, respectively. However, there are no positive signals in either glomerulus or PCT. **a'** (*inset* of **a** at the higher magnification): Immunoreactivity in CTAL (*arrows*) and MD (*white arrowheads*). Boundaries of CTAL and each MD cell are drawn by *dashed* and *dotted lines*, respectively. **b** Immunoreactive signals are positive in CCD (*arrowheads*) and CTAL (*arrows*). Note that signals are moderate and heterogeneous in the CCD, whereas they are strong and homogeneous in the CTAL. Boundaries of the tubules are drawn by *dashed lines*. **c** Immunoreactive signals are positive in MTAL (*arrows*), but are negative in OMCD. *Scale bars* 10 μm. **d, e** Quantitative analysis of CaSR mRNA expression per tubule (50 μm in length) and per cell of each nephron segment. Note that the average number of signals in the positive cells of the CCD are as high as those of the TALs and MD. No estimation was conducted in MD due to its short length (# in Fig. 1d). $n = 10$ each

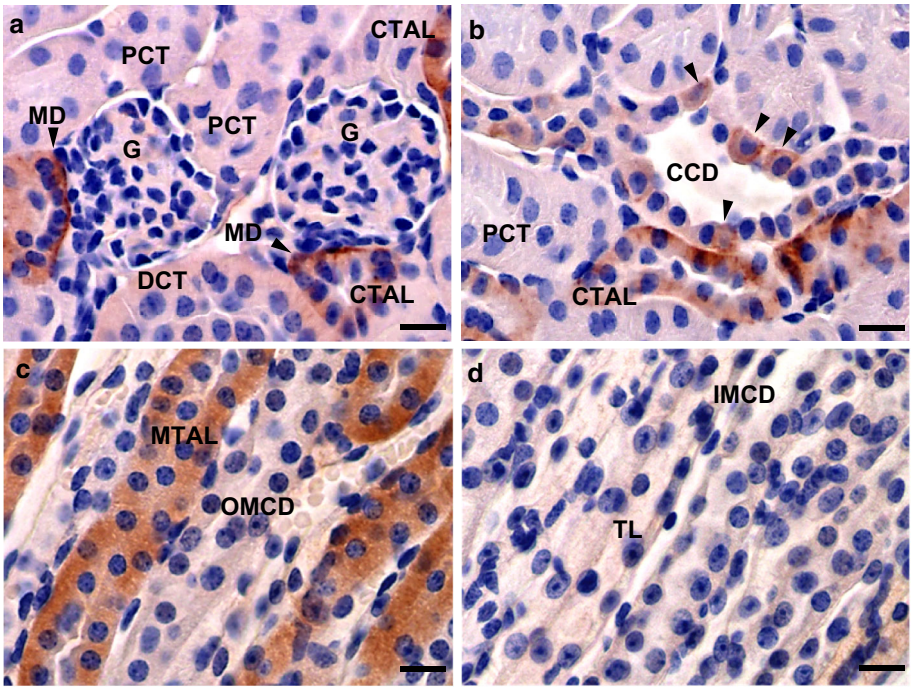

Fig. 2 DAB-staining immunohistochemistry in mouse kidney. **a** Positive immunostainings are strong in MD, moderate in CTAL, and weak in DCT. No staining in either glomerulus (G) or PCT. Note the clear basolateral staining in MD (*arrowheads*). **b** Relatively homogeneous staining in CTAL, whereas heterogeneous staining in CCD (*arrowheads*). **c** Strong, homogeneous staining in MTAL. No staining in OMCD. **d** No staining in either TL or IMCD. *Scale bars* 10 μm

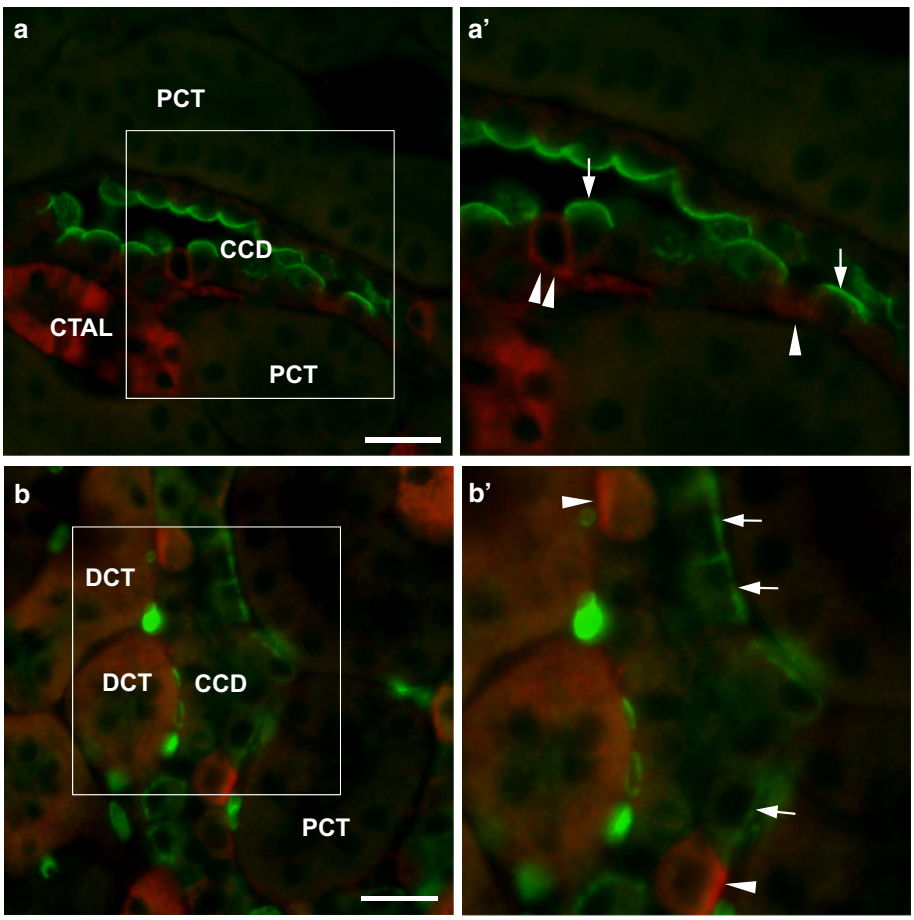

Fig. 3 Expression and localization of CaSR in the CCD. Kidney cortex was labeled with antibodies against the PC-specific water channel AQP2 (*green*, **a, a'**) and against the IC-A specific AE1 (*green*, **b, b'**) as well as with an antibody against CaSR (*red*). **a, a'** CaSR signals were strongly and moderately stained, respectively, in CTAL and in the CCD (*inset*). CaSR is expressed as a "ring-like structure" (double arrowhead) and a "barrel-like structure" (*arrowheads*) and is not co-expressed in AQP2-positive (*green*) cells. No expression of CaSR in the PCT. **b** CaSR is not co-expressed in AE1-positive (*green*), basolateral staining cells. *Inset*: CaSR staining (*red*) is more intense in the basolateral membrane (*arrowheads*). Clear, but faint staining of AE1 (*green*) in the basolateral membrane (*arrows*). *Scale bars* 20 μm

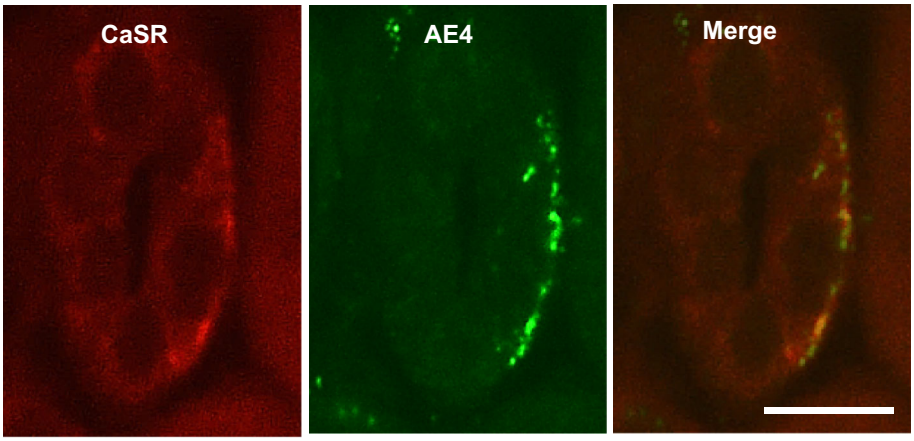

Fig. 4 Representative immunofluorescence images of CaSR and AE4 in the kidney CCD cells. Double-label immunofluorescence showing CaSR (*red*), AE4 (*green*), and a merged image, as indicated. Note colocalization of CaSR and AE4 in the basolateral membrane of IC-B (AE4 positive cell). *Scale bars* 10 μm

Table 1 Blood data

	Control (6)	+NH_4Cl (6)	+$NaHCO_3$ (6)
pH	7.39 ± 0.03	7.19 ± 0.01**	7.38 ± 0.01
pCO_2, mmHg	31.9 ± 2.5	28.2 ± 1.0	34.5 ± 1.1
pO_2, mmHg	152.6 ± 3.4	158.3 ± 1.3	154.6 ± 2.0
HCO_3^-, mM	18.8 ± 0.9	10.4 ± 0.3**	20.0 ± 0.7
Na^+, mM	144.6 ± 0.9	148.0 ± 0.6	146.3 ± 1.3
K^+, mM	3.7 ± 0.1	4.5 ± 0.1**	4.1 ± 0.1
Cl^-, mM	115.4 ± 0.7	127.2 ± 0.5**	118.0 ± 0.9
Ca^{2+}, mg/dl	7.5 ± 0.3	7.7 ± 0.2	7.9 ± 0.1
Osmolality, mOsm/kg H_2O	308.8 ± 1.0	323.3 ± 0.8**	323.7 ± 1.4

Values are mean ± SE

** $P < 0.005$ vs. control

Table 2 Urine data

	Control (6)	+NH_4Cl (6)	+$NaHCO_3$ (6)
pH	6.50 ± 0.06	5.96 ± 0.03**	8.87 ± 0.07**
Fluid intake, ml/day	4.9 ± 0.3	8.0 ± 0.3**	8.4 ± 0.2**
Volume, ml/day	1.0 ± 0.2	1.9 ± 0.3*	1.8 ± 0.2**
Na^+, μmol/day	209.7 ± 21.7	293.8 ± 46.6	1136.4 ± 90.7**
K^+, μmol/day	375.1 ± 41.6	471.1 ± 51.1	499.6 ± 44.4*
Cl^-, μmol/day	389.1 ± 39.1	1220.2 ± 145.4**	579.3 ± 57.7*
Ca^{2+}, mg/day	51.3 ± 10.0	154.7 ± 22.0**	56.1 ± 5.6
Osmolality, mOsm/kgH_2O	3808 ± 525	2627 ± 216*	3007 ± 208

Values are mean ± SE

* $P < 0.05$, ** $P < 0.005$ vs. control

and CCD cells after acid/base diets (referred to cell-height measurement in "Materials and methods" and Fig. 5a–c and the insets). In the CTAL and the PC of CCD, there was no significant change in cell-heights 6 days after the NH_4Cl- and $NaHCO_3$-loading (Fig. 7a, b). As expected, NH_4Cl-loading induced significant hypertrophy in IC-A ($P < 0.005$) (Fig. 7c), while $NaHCO_3$-loading induced significant hypertrophy in IC-B ($P < 0.005$) (Fig. 7d).

Acute influence of furosemide and neomycin

In the final series of experiments, we investigated time-dependent changes of several urine parameters when mice were injected with either furosemide (an inhibitor of NKCC2 in TAL) or neomycin (an agonist of CaSR). Hourly urine volume (UV) and excretion of Ca significantly increased 1 h after furosemide injection ($P < 0.005$ and $P < 0.05$, respectively, unpaired Student's t test) (Fig. 8a, e), however, urine [Ca^{2+}] and pH were almost unaffected for 3 h (Fig. 8c, g). On the other hand, although urine flow was significantly unchanged after injection of neomycin (Fig. 8b), both urine [Ca^{2+}] and hourly Ca excretion increased significantly ($P < 0.005$, unpaired Student's t test) in the first 1-h urine (Fig. 8d, f). More importantly, urine pH started to decrease in the first 1-h period after injection ($P < 0.05$, unpaired Student's t test) and further decreased in the second and third 1 h (Fig. 8h).

Moreover, we investigated time-dependent changes of urine Pi and Mg after injection of neomycin for 2 h. Although the values varied time-dependently during the experimental period [Pi (μg/h) (cont: 48.2 ± 9.9 ∼ 118.1 ± 19.5; neomycin: 69.5 ± 20.3 ∼ 121.2 ± 25.2); Mg (μg/h) (cont: 28.7 ± 3.5 ∼ 68.0 ± 13.7; neomycin: 21.4 ± 2.5 ∼ 73.5 ± 15.4)], there was no significant difference between the two groups at each corresponding time ($n = 9$ each group, two-way ANOVA; unpaired Student's t test).

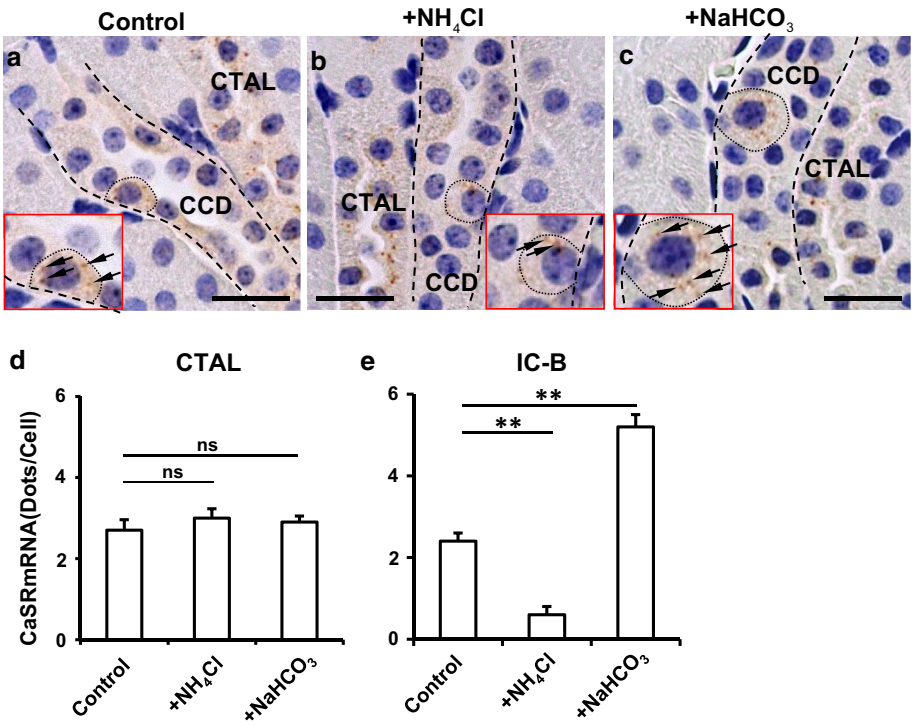

Fig. 5 Quantitative analysis of CaSR mRNA signals in the CCD. Dots of CaSR mRNA signal in control (**a**), NH_4Cl loading (**b**), and $NaHCO_3$ loading (**c**). Boundaries of CCD and each IC-B cell are illustrated by *dashed* and *dotted lines*, respectively. *Scale bars* 20 μm. **a, b, c** *insets* provide more reliable images of IC-B at the higher magnification. **d** No acid/base dependent expression was observed in the CTAL. **e** Conversely, note that the levels of the CaSR expression in IC-B were decreased and increased significantly ($P < 0.005$) in mice fed NH_4Cl (acid) and $NaHCO_3$ (alkali) diets, respectively, for 6 days, $n = 10$ for each condition

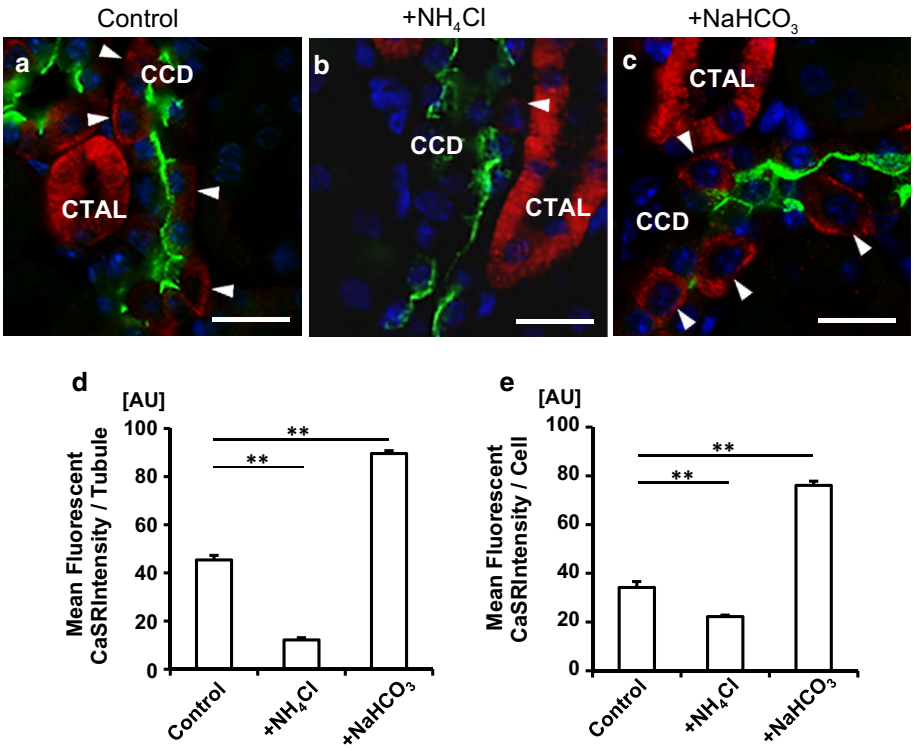

Fig. 6 Quantitative analysis of CaSR protein in CCD. **a, b, c** Immunofluorescence of CaSR (*red*)(*arrowheads*) and AQP2 (*green*) in control (**a**), NH_4Cl loading (**b**), and $NaHCO_3$ loading (**c**). Immunofluorescent intensity of CaSR (*red*) in CTAL was strong and unchanged in the present experimental condition (**a–c**). Conversely, it was decreased (**b**) and increased (**c**) in IC-B. *Scale bars* 20 μm. **d, e** All data were normalized to the intensity of CaSR immunoreactivity in the CTAL at the corresponding experimental condition. Relative intensity of CCD per tubule (**d**) and per IC-B cell (**e**). $n = 10$ for each condition

Discussion

In the present study, we found that the mouse calcium-sensing receptor (CaSR), originally cloned from rat kidney [9], was specifically expressed in the basolateral membrane of mouse kidney CCD type-B intercalated cells (IC-B) as well as MTAL, CTAL, MD, and DCT. CaSR was not found in glomeruli, PCT, PST, TL, OMCD, or in IMCD. These observations are essentially consistent with the previous work with RT-PCR in the rat kidney nephron

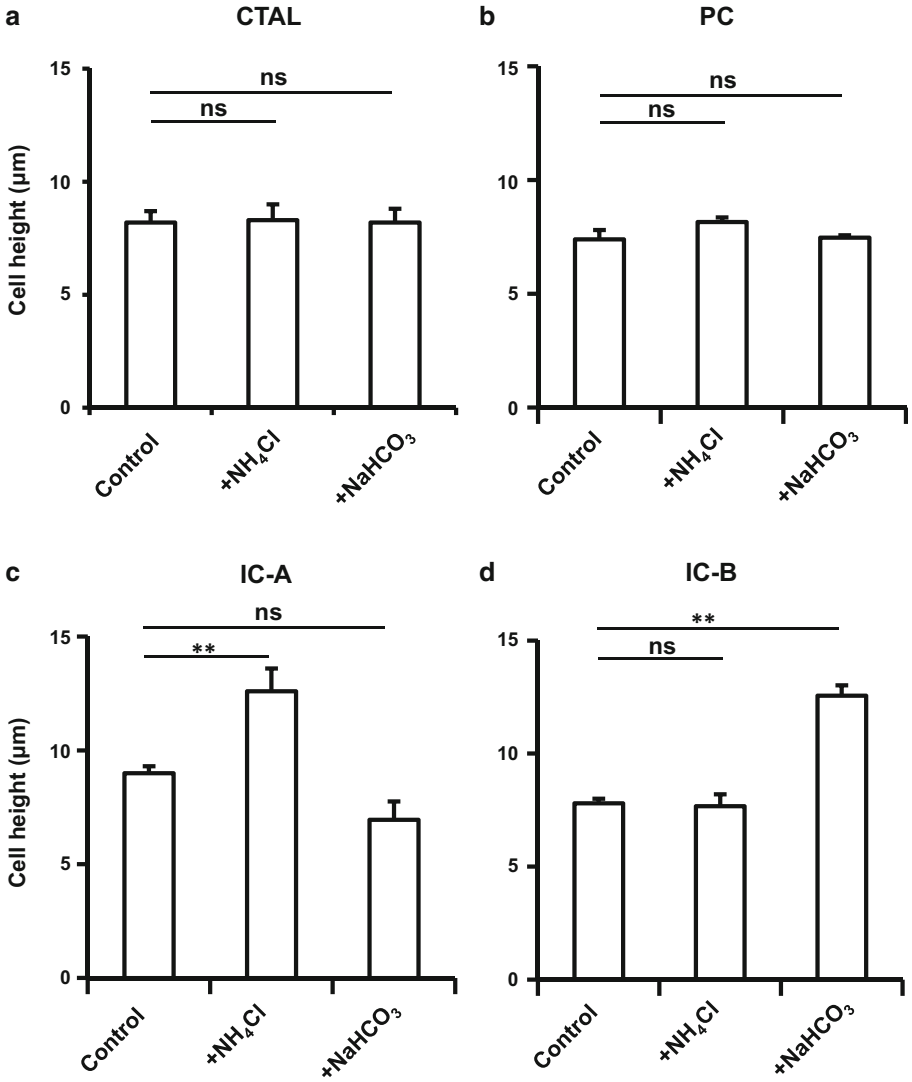

Fig. 7 The effects of acid or alkali on cell height in CTAL and CCD. **a, b** Cell heights of the CTAL and the PC of the CCD were unchanged in the present experimental condition. **c, d** Conversely, the cell heights of IC-A and IC-B increased significantly ($P < 0.005$) when mice were fed NH_4Cl (acid) and $NaHCO_3$ (alkali) diets, respectively, for 6 days. $n = 10$ for each condition

[14], however, inconsistent with those of Riccardi et al. [13]. They reported that the CaSR protein was expressed in rat kidney PCT, PST, DCT, IC-A of CCD as well as MTAL and CTAL and that it was mainly localized to the apical membrane of PCT [13] and IMCD [11, 13]. Importantly, we would like to point out that according to their original data shown in Fig. 1A of Riccardi et al. [10], CaSR (RaKCaR) mRNA does not appear to be expressed along virtually the entire nephron, from glomeruli to IMCD, but rather shows an expression pattern resembling the zonal expression pattern observed in this study. Moreover, recent immunohistochemical studies in rats [15] and mice [16] showed that the CaSR protein was not detected in the PCT, DCT, or CDs. However, in Fig. 3 of Toka et al. [16] we have found clear, heterogeneous staining of CaSR signals in CCD.

The antibodies except AE1 and AE4 used in the present study are the same as those used in the previous manuscript [26]. There are several studies which show that localization of AE4 in the kidney varies between species. Blomqvist et al. [28], Chambrey et al. [31], and Purkerson et al. [32] showed basolateral membrane staining of the anti AE4 antibody (Alpha Diagnostics) in mouse and rabbit IC-B. On the other hand, Tsuganezawa et al. [33], Ko et al. [34], and Xu et al. [35] showed the species different localization patterns in kidney tubule cells. AE4 was localized to the apical membrane of IC-B in the rabbit [33, 35], and in another study, to rabbit kidney IC-A (apical, lateral), rat kidney IC-A (basolateral), and mouse kidney CCD (basolateral) [34].

According to the study of Purkerson et al. [32], AE4 (SLC4a9) is expressed as a "barrel-like structure" in the basolateral membrane of IC-B, and its expression levels are decreased under acid loading and increased during alkali loading. An occasional apparent apical distribution (ring-like pattern) was also observed in Purkerson et al. [32] and

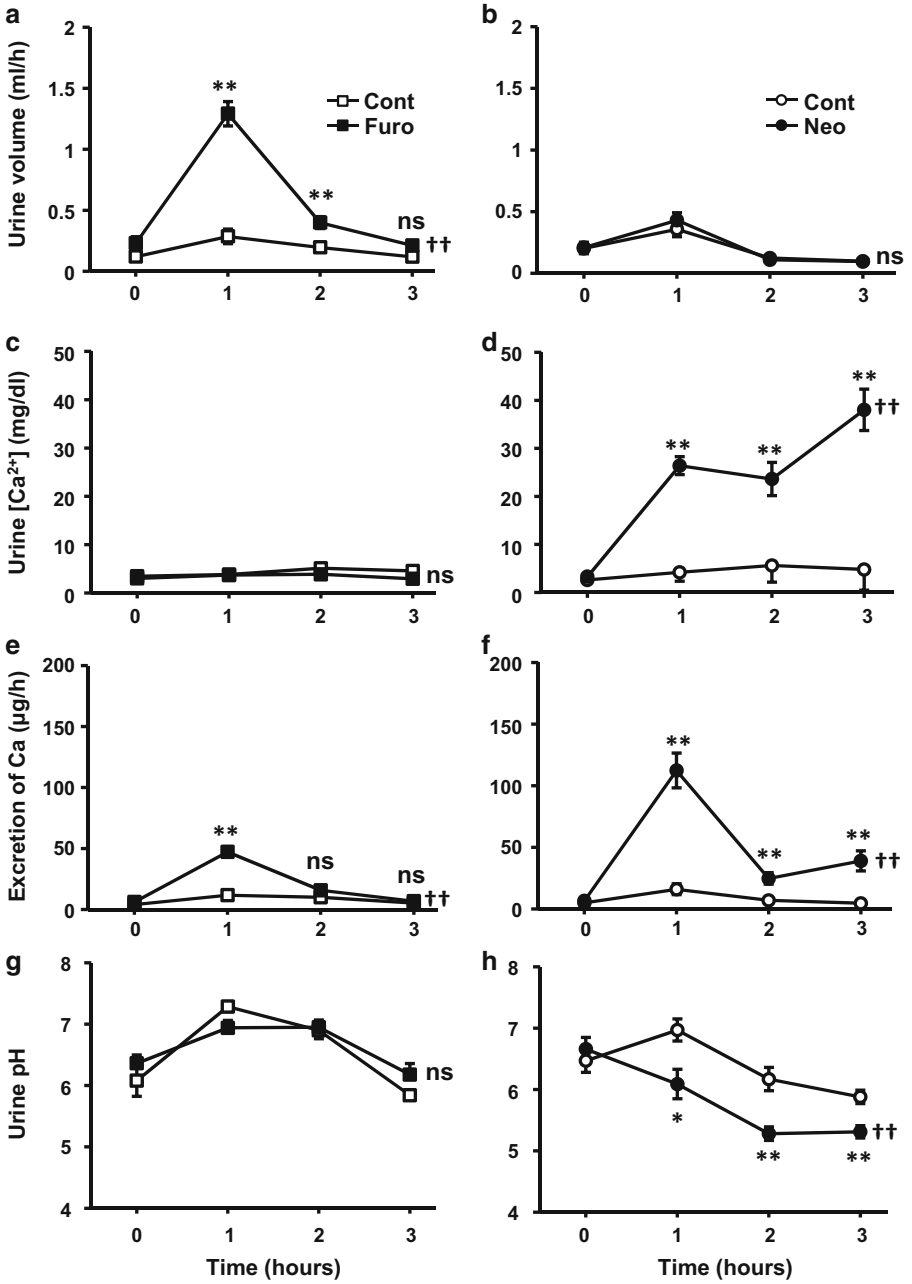

Fig. 8 Time-dependent changes in urine parameters after single-infusion (ip) of either furosemide or neomycin. **a, b** Hourly urine volume. **c, d** Urine Ca concentration ($[Ca^{2+}]$). **e, f** Hourly excretion of Ca. **g, h** Urine pH. Note that single-infusion of neomycin significantly increased urine $[Ca^{2+}]$ and urinary Ca excretion ($^{\dagger\dagger}P < 0.005$, two-way ANOVA) and decreased urine pH ($^{\dagger}P < 0.05$, two-way ANOVA). $n = 7$–10 for each condition. Significance assessed between the different animal groups at the corresponding time was performed by unpaired Student's t test ($^{**}P < 0.005$)

is shown in Fig. 3a', b' in the present study. More positive staining was detected on the basolateral membrane of IC-B at least in mouse kidney.

The CaSR, expressed in all vertebrates including fishes, is known to conserve the common molecular structure of a dimeric seven transmembrane, G-protein-coupled receptor [8, 36]. The CaSR in endocrine tissues functions as a sensor of extracellular Ca concentration ($[Ca^{2+}]_o$) in the context of systemic Ca homeostasis, whereas CaSR in ion transporting tissues, such as kidney, intestine, gills, and rectal glands, may contribute to the regulation of water and ion transport across the epithelia as a sensor of $[Ca^{2+}]_o$. Interestingly, there is general agreement that in the kidney CaSR expressed on the basolateral membrane of the medullary and cortical TAL regulates Ca reabsorption by sensing $[Ca^{2+}]_o$ [4, 8, 37, 38]. However, CaSR localization along the nephron except the TAL is controversial and its role in the nephron except the TAL is still unknown.

Some studies suggested that CaSR in the apical membrane of PC and IC-A, respectively, might protect against urolithiasis by inhibiting AQP2 in the apical membrane of PC (thus increasing urine flow) and stimulating the proton pump in the apical membrane of IC-A (thus enhancing urinary acidification) [38, 39]. However, in refutation of

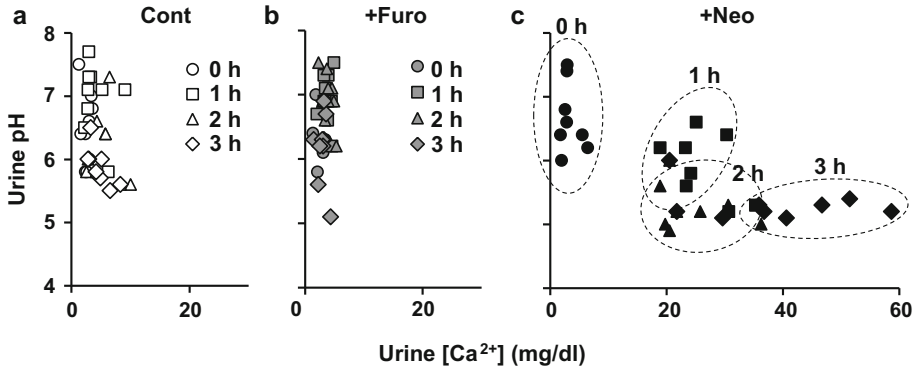

Fig. 9 Relationships between urine [Ca^{2+}] and pH after single-infusion of either furosemide or neomycin. **a, b** No time-dependent changes are observed in control or after furosemide injection. **c** Conversely, following neomycin injection urine [Ca^{2+}] increased after 1 h. Urine pH started to decrease at 1 h and further decreased at 2 and 3 h after neomycin injection

the above, no detectable urinary acidification or increased urine flow was observed in patients with genetic hypercalciuria [40].

We also analyzed acute, time-dependent changes in the relationship between urinary [Ca^{2+}] and urine pH after single-infusion (ip) of either furosemide or neomycin (Fig. 9a–c). In the present study, we initially expected that urine would be alkalinized after infusion of neomycin. However, after infusion of neomycin, urinary [Ca^{2+}] was increased at first as was the excretion of Ca (Fig. 8d, f) and then, this resulted in urinary acidification in the similar time-course (Fig. 8h). This clearly supports the idea that neomycin inhibited Ca reabsorption via stimulation of basolateral CaSR in TAL and then acidified the urine via unknown mechanism in the CCD. These observations in the present study very much agree with the recent observation by Casare et al. [17] and support the idea that unidentified CaSR may function in the CCD.

Quinn et al. [23] showed that in cultured kidney 293 cells the sensitivity of CaSR decreased at extracellular acidic pH and increased at extracellular alkaline pH. Further, the extracellular pH modulates the response of this receptor to both Ca^{2+} and Mg^{2+} [41]. These results suggest that CaSR may be a candidate for a signaling pH sensor in the CCD. In the present study, we showed that the level of the CaSR mRNA and protein expression in IC-B significantly decreased under acid-loading conditions and increased under alkali-loaded conditions. The pH-sensitive expression of CaSR in IC-B, in collaboration with pH-sensitive activity of CaSR [23], could amplify the external signal of pH and ionic concentrations, when mice are loaded with acid and alkali containing diets. This pH sensitivity may additionally and effectively regulate the bicarbonate excretion into the urine. These properties of CaSR may be essential to stimulate the alkali and acid excretion to the urine when mice are treated for 6 days with alkali- and acid-containing diets. Localization of CaSR in IC-B, and NOT in IC-A, is in keeping with a role in regulating the systemic acid and alkali balance. Coordinate regulation of pendrin (apical HCO_3^-/Cl^- transporter) and AE4 (basolateral HCO_3^-/Cl^- transporter) in IC-B has very recently been reported in rabbit kidney [32].

In conclusion, a basolateral type of CaSR expressed in the TAL was also localized in the basolateral membrane of IC-B in the mouse kidney CCD. Its expression was stimulated and inhibited by alkali- and acid-containing diets.

Acknowledgments This study was supported by grants from the Grants-in-Aid for Scientific Research from the Ministry of Education, Culture, Sports, Science and Technology of Japan to Y.Y. (No. 24790222) and to K.K. (No. 23591224, 26461259). Special thanks are given to Y.Nakabayashi (Kitasato Univ Sch of Med) for her technical assistance. Parts of this study were presented at the meetings of American Society of Nephrology (Philadelphia, 2011) and International Union of Physiological Sciences (Birmingham (UK), 2013).

Conflict of interest The authors have declared that no conflict of interest exists.

References

1. Fenton RA, Knepper MA. Mouse models and the urinary concentrating mechanism in the new millennium. Physiol Rev. 2007;87:1083–112.
2. Wang WH, Giebisch G. Regulation of potassium (K) handling in the renal collecting duct. Pflügers Arch. 2009;458:157–68.
3. Staruschenko A. Regulation of transport in the connecting tubule and cortical collecting duct. Compr Physiol. 2012;2:1541–84.
4. Hebert SC, Brown EM, Harris HW. Role of the Ca^{2+}-sensing receptor in divalent mineral ion homeostasis. J Exp Biol. 1997;200:295–302.
5. Brown EM, Gamba G, Riccardi D, Lombardi M, Butters R, Kifor O, Sun A, Hediger MA, Lytton J, Hebert SC. Cloning and characterization of an extracellular Ca^{2+}-sensing receptor from bovine parathyroid. Nature. 1993;366:575–80.
6. Brown EM, Pollak M, Riccardi D, Hebert SC. Cloning and characterization of an extracellular Ca^{2+}-sensing receptor from parathyroid and kidney: new insights into the physiology and pathophysiology of calcium metabolism. Nephrol Dial Transplant. 1994;9:1703–6.
7. Houillier P. Calcium-sensing in the kidney. Curr Opin Nephrol Hypertens. 2013;22:566–71.
8. Alfadda TI, Saleh AM, Houillier P, Geibel JP. Calcium-sensing receptor 20 years later. Am J Physiol Cell Physiol. 2014;307:C221–31.

9. Riccardi D, Park J, Lee WS, Gamba G, Brown EM, Hebert SC. Cloning and functional expression of a rat kidney extracellular calcium/polyvalent cation-sensing receptor. Proc Natl Acad Sci USA. 1995;92:131–5.
10. Riccardi D, Lee WS, Lee K, Segre GV, Brown EM, Hebert SC. Localization of the extracellular Ca^{2+}-sensing receptor and PTH/PTHrP receptor in rat kidney. Am J Physiol. 1996;271:F951–6.
11. Chattopadhyay N, Baum M, Bai M, Riccardi D, Hebert SC, Harris HW, Brown EM. Ontogeny of the extracellular calcium-sensing receptor in rat kidney. Am J Physiol. 1996;271:F736–43.
12. Sands JM, Naruse M, Baum M, Jo I, Hebert SC, Brown EM, Harris HW. Apical extracellular calcium/polyvalent cation-sensing receptor regulates vasopressin-elicited water permeability in rat kidney inner medullary collecting duct. J Clin Invest. 1997;99:1399–405.
13. Riccardi D, Hall AE, Chattopadhyay N, Xu JZ, Brown EM, Hebert SC. Localization of the extracellular Ca^{2+}/polyvalent cation-sensing protein in rat kidney. Am J Physiol. 1998;274:F611–22.
14. Yang T, Hassan S, Huang YG, Smart AM, Briggs JP, Schnermann JB. Expression of PTHrP, PTH/PTHrP receptor, and Ca^{2+}-sensing receptor mRNAs along the rat nephron. Am J Physiol. 1997;272:F751–8.
15. Loupy A, Ramakrishnan SK, Wootla B, Chambrey R, de la Faille R, Bourgeois S, Bruneval P, Mandet C, Christensen EI, Faure H, Cheval L, Laghmani K, Collet C, Eladari D, Dodd RH, Ruat M, Houillier P. PTH-independent regulation of blood calcium concentration by the calcium-sensing receptor. J Clin Invest. 2012;122:3355–67.
16. Toka HR, Al-Romaih K, Koshy JM, DiBartolo S 3rd, Kos CH, Quinn SJ, Curhan GC, Mount DB, Brown EM, Pollak MR. Deficiency of the calcium-sensing receptor in the kidney causes parathyroid hormone-independent hypocalciuria. J Am Soc Nephrol. 2012;23:1879–90.
17. Casare F, Milan D, Fernandez R. Stimulation of calcium-sensing receptor increases biochemical H^+-ATPase activity in mouse cortex and outer medullary regions. Can J Physiol Pharmacol. 2014;92:181–8.
18. Kerstens HM, Poddighe PJ, Hanselaar AG. A novel in situ hybridization signal amplification method based on the deposition of biotinylated tyramine. Histochem Cytochem. 1995;43:347–52.
19. Suzuki T, Kadoya Y, Sato Y, Handa K, Takahashi T, Kakita A, Yamashina S. The expression of pancreatic endocrine markers in centroacinar cells of the normal and regenerating rat pancreas: their possible transformation to endocrine cells. Arch Histol Cytol. 2003;66:347–58.
20. Kobayashi M, Yasuoka Y, Sato Y, Zhou M, Abe H, Kawahara K, Okamoto H. Upregulation of calbindin D28k in the late distal tubules in the potassium-loaded adrenalectomized mouse kidney. Clin Exp Nephrol. 2011;15:355–62.
21. Kriz W, Bankir L. A standard nomenclature for structures of the kidney. Kidney Int. 1988;33:1–7.
22. Madsen KM, Tisher CC. Response of intercalated cells of rat outer medullary collecting duct to chronic metabolic acidosis. Lab Invest. 1984;51:268–76.
23. Quinn SJ, Bai M, Brown EM. pH sensing by the calcium-sensing receptor. J Biol Chem. 2004;279:37241–9.
24. Ikebe M, Nonoguchi H, Nakayama Y, Tashima Y, Tomita K. Upregulation of the secretory-type $Na^+/K^+/2Cl^-$-cotransporter in the kidney by metabolic acidosis and dehydration in rats. J Am Soc Nephrol. 2001;12:423–30.
25. Wagner CA, Finberg KE, Stehberger PA, Lifton RP, Giebisch GH, Aronson PS, Geibel JP. Regulation of the expression of the Cl^-/anion exchanger pendrin in mouse kidney by acid-base status. Kidney Int. 2002;62:2109–17.
26. Yasuoka Y, Kobayashi M, Sato Y, Nonoguchi H, Tanoue A, Okamoto H, Kawahara K. Decreased expression of aquaporin 2 in the collecting duct of mice lacking the vasopressin V1a receptor. Clin Exp Nephrol. 2013;17:183–90.
27. Sumida K, Nakamura M, Ubara Y, Marui Y, Tanaka K, Takaichi K, Tomikawa S, Inoshita N, Ohashi K. Cinacalcet upregulates calcium-sensing receptors of parathyroid glands in hemodialysis patients. Am J Nephrol. 2013;37:405–12.
28. Blomqvist SR, Vidarsson H, Fitzgerald S, Johansson BR, Ollerstam A, Brown R, Persson AEG, Bergström G, Enerbäck S. Distal renal tubular acidosis in mice that lack the forkhead transcription factor Foxi1. J Clin Invest. 2004;113:1560–70.
29. Yasuoka Y, Kobayashi M, Sato Y, Zhou M, Abe H, Okamoto H, Nonoguchi H, Tanoue A, Kawahara K. The intercalated cells of the mouse kidney $OMCD_{is}$ are the target of the vasopressin V1a receptor axis for urinary acidification. Clin Exp Nephrol. 2013;17:783–92.
30. Wall SM, Hassell KA, Royaux IE, Green ED, Chang JY, Shipley GL, Verlander JW. Localization of pendrin in mouse kidney. Am J Physiol Renal Physiol. 2003;284:F229–41.
31. Chambrey R, Kurth I, Peti-Peterdi J, Houillier P, Purkerson JM, Leviel F, Hentschke M, Zdebik AA, Schwartz GJ, Hübner CA, Eladari D. Renal intercalated cells are rather energized by a proton than a sodium pump. Proc Natl Acad Sci USA. 2013;110:7928–33.
32. Purkerson JM, Heintz EV, Nakamori A, Schwartz GJ. Insights into acidosis-induced regulation of SLC26A4 (pendrin) and SLC4A9 (AE4) transporters using three-dimensional morphometric analysis of β-intercalated cells. Am J Physiol Renal Physiol. 2014;307:F601–11.
33. Tsuganezawa H, Kobayashi K, Iyori M, Araki T, Koizumi A, Watanabe S, Kaneko A, Fukao T, Monkawa T, Yoshida T, Kim DK, Kanai Y, Endou H, Hayashi M, Saruta T. A new member of the HCO_3^- transporter superfamily is an apical anion exchanger of β-intercalated cells in the kidney. J Biol Chem. 2001;276:8180–9.
34. Ko SB, Luo X, Hager H, Rojek A, Choi JY, Licht C, Suzuki M, Muallem S, Nielsen S, Ishibashi K. AE4 is a DIDS-sensitive Cl^-/HCO_3^- exchanger in the basolateral membrane of the renal CCD and the SMG duct. Am J Physiol Cell Physiol. 2002;283:C1206–18.
35. Xu J, Barone S, Petrovic S, Wang Z, Seidler U, Riederer B, Ramaswamy K, Dudeja PK, Shull GE, Soleimani M. Identification of an apical Cl^-/HCO_3^- exchanger in gastric surface mucous and duodenal villus cells. Am J Physiol Gastrointest Liver Physiol. 2003;285:G1225–34.
36. Loretz CA. Extracellular calcium-sensing receptors in fishes. Comp Biochem Physiol A Mol Integr Physiol. 2008;149:225–45.
37. Brown EM, MacLeod RJ. Extracellular calcium sensing and extracellular calcium signaling. Physiol Rev. 2001;81:239–97.
38. Riccardi D, Brown EM. Physiology and pathophysiology of the calcium-sensing receptor in the kidney. Am J Physiol Renal Physiol. 2010;298:F485–99.
39. Renkema KY, Velic A, Dijkman HB, Verkaart S, van der Kemp AW, Nowik M, Timmermans K, Doucet A, Wagner CA, Bindels RJ, Hoenderop JG. The calcium-sensing receptor promotes urinary acidification to prevent nephrolithiasis. J Am Soc Nephrol. 2009;20:1705–13.
40. Bergsland KJ, Coe FL, Gillen DL, Worcester EM. A test of the hypothesis that the collecting duct calcium-sensing receptor limits rise of urine calcium molarity in hypercalciuric calcium kidney stone formers. Am J Physiol Renal Physiol. 2009;297:F1017–23.
41. Brown D, Wagner CA. Molecular mechanisms of acid-base sensing by the kidney. J Am Soc Nephrol. 2012;23:774–80.